Electronic Supplementary Material (ESI) for Soft Matter.

DC electric field-driven heartbeat phenomenon of gallium-based liquid metal on a floating electrode

Zhenyou Ge[a], Ye Tao*[ab], Weiyu Liu[c], Chunlei Song[a], Rui Xue[a] , Hongyuan Jiang[d], Yukun Ren*[a]

[a.] *State Key Laboratory of Robotics and System, Harbin Institute of Technology, West Da-zhi Street 92, Harbin, Heilongjiang 150001, People's Republic of China.*

[b.] *School of Engineering and Applied Sciences and Department of Physics Harvard University, 9 Oxford Street, Cambridge, MA 02138, USA.*

[c.] *Chang'an University, Middle-Section of Nan'er Huan Road, Xi'an 710000, China*

[d.] *School of Mechatronics Engineering, Harbin Institute of Technology, West Da-zhi Street 92, Harbin 150001, People's Republic of China.*

* *Corresponding author.*

E-mail addresses: ytao@seas.harvard.edu (Ye Tao)

rykhit@hit.edu.cn (Yukun Ren)

Supplementary Information Appendix

SI Appendix 1: The influence of heart beating on the graphite surface.

After 5 minutes of heartbeat, there were some changes on the surface of the graphite floating electrode. By comparing the scanning electron microscope (SEM) images under the same conditions, the graphite surface after the heartbeat was flatter (shown in Fig.S1(a) and S1(b)). This may be due to the collision between the LMD and the graphite surface to remove the protrusions. Energy dispersive X-ray (EDX) studies were carried out to demonstrate the surface elemental composition of the graphite after the heartbeat, as shown in Fig. S1(c). There were 2.80% Na and 2.44% Ga elements by weight on the graphite surface after the experiment, as shown in Fig.S1(d). This suggested that the graphite surface adsorbed Na and Ga elements during the heartbeat process, which provided indirect evidence that there was a certain interaction between LMD and graphite.

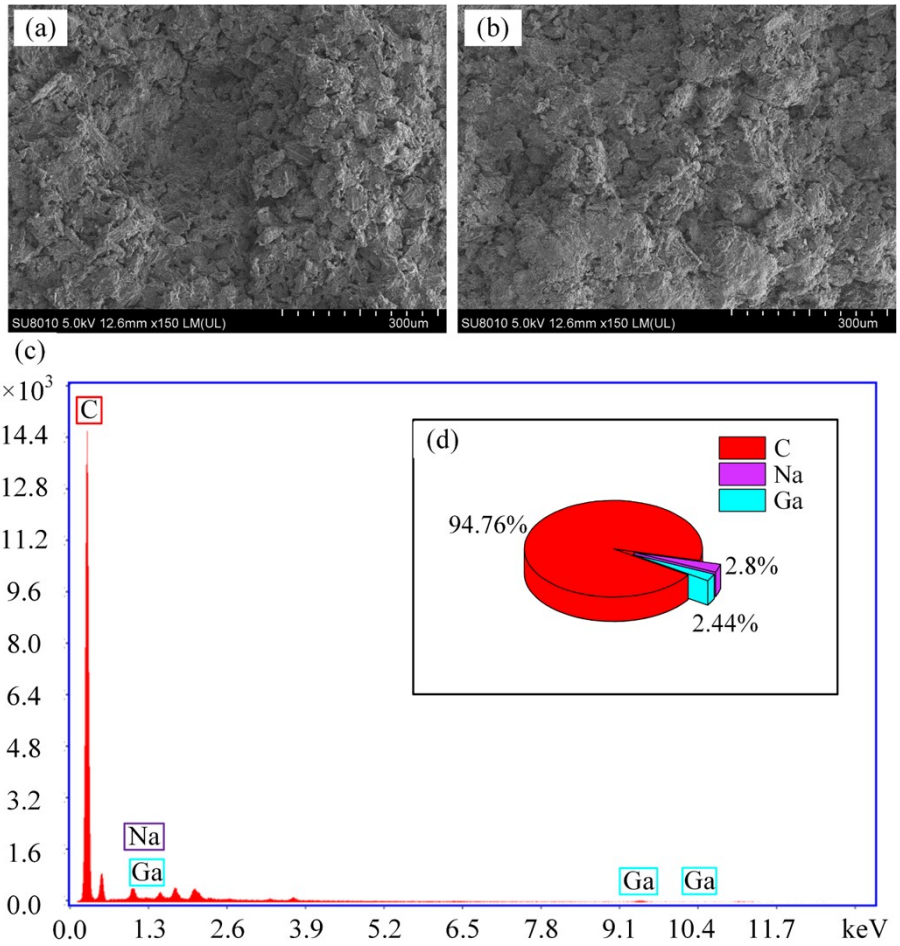

Fig. S1 The comparison of graphite floating electrodes before and after the heartbeat. (a) SEM image of the graphite before the heartbeat. (b) SEM image of the graphite after the heartbeat. (c) EDX elemental analysis of the graphite after the heartbeat. (d) The proportion by weight of each element on the graphite surface.

SI Appendix 2: The surface charge distribution of liquid metal droplet

When the liquid metal droplet (LMD) was stationary in the NaOH solution, a

native electric double layer (NDL) was formed on the surface of the droplet, as shown in Fig.S2(a). The NDL charges were evenly distributed along the surface of the LMD. When the DC voltage was applied to both ends of the LMD, an induced electric double layer (IDL) was formed on the surface of the droplet, as shown in Fig.S2(b). Charges of opposite polarity were induced on the left and right sides of the LMD, and IDL charges presented dipole distribution characteristics.

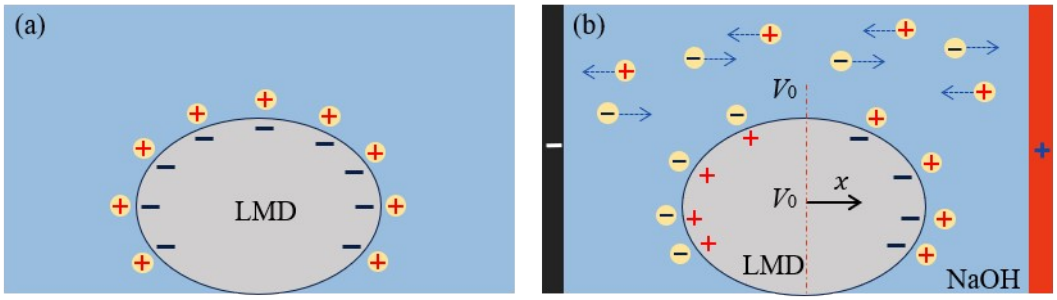

Fig. S2 The surface charge distribution of LMD under different conditions. (a) The native charge distribution on the surface when no electric field was applied. (b) The induce charge distribution on the surface when the DC voltage was applied.

When the graphite floating electrode was immersed in the NaOH solution, the opposite charge distribution was formed on the floating electrode as the center under the induction of the electric field, as shown in Fig.S3. The LMD contacted the graphite floating electrode and formed a unified conductor. And a positive charge distribution gradient was induced under the action of the electric field. Define the internal potential of the floating electrode as V_0 and the length of the floating electrode in the x-direction as L. By taking the center of the droplet as the origin of the x coordinate and pointing to the positive electrode as the positive direction, the surface potential of the droplet can be calculated.

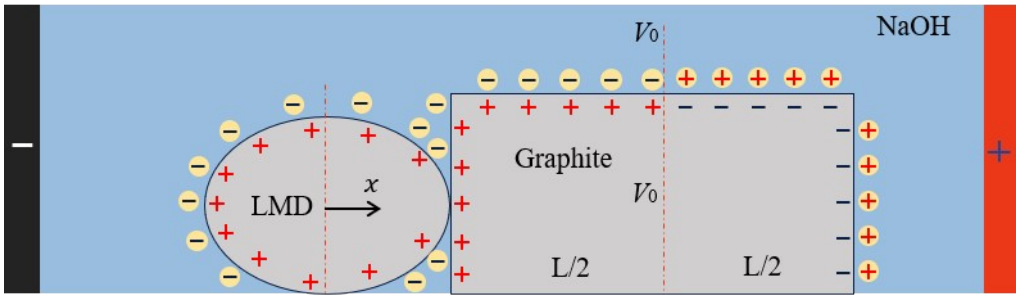

Fig. S3 The induced charge distribution on the surface of the droplet and graphite when the droplet contacted the graphite floating electrode.

SI Appendix 3: CEW of EGaIn in alkaline solution

Due to the force equilibrium between electrostatic attraction and thermal diffusion, the voltage drop across the NDL was ΔV_1:

$$\Delta V_1 = -\frac{q_0}{C} \tag{S1}$$

where q_0 is the inherent surface charge density adsorbed on the conductive droplet,

$C = \varepsilon / \lambda_D$ the EDL capacitance, ε the liquid permittivity, $\lambda_D = \sqrt{D\varepsilon / \sigma}$ the Debye screening length, D the ion diffusivity at room temperature, and σ the medium electric conductivity.

The induced electric charges on the left and right sides of the LM had opposite polarities and the characteristics of dipole distribution. The voltage drop across the IDL was approximately ΔV_2.

$$\Delta V_2 = V_0 - (V_0 + Ex) = -Ex \tag{S2}$$

where V_0 is the internal potential of the LM body, E is the electric field strength in the solution. The x-coordinate is centered on the LM and positive in the direction of the electric field (shown in Fig.S2(b)).

The full voltage drop expression of the EDL was ΔV:

$$\Delta V = \Delta V_1 + \Delta V_2 = -\frac{q_0}{C} - Ex \tag{S3}$$

The interfacial tension was related to the voltage drop across the EDL, according to the Lippmann equation:

$$\gamma = \gamma_0 - \frac{1}{2} \cdot C \cdot (\Delta V)^2 \tag{S4}$$

where γ is the interfacial tension, γ_0 is the maximum interfacial tension at ΔV=0.

As long as the LMD can move freely without any space constraints, the fluid physics in CEW is a transient two-phase flow problem driven by the surface stress of the electrocapillary at the metal/electrolyte interface. The flow behavior of incompressible Newtonian fluid is controlled by the Navier Stokes equation:

$$\rho \nabla \cdot \boldsymbol{u} = 0 \tag{S5}$$

$$\rho \frac{\partial u}{\partial t} + \rho(\boldsymbol{u} \cdot \nabla)\boldsymbol{u} = \nabla \cdot [-p + \eta \nabla \boldsymbol{u}] + \boldsymbol{F} \tag{S6}$$

where ρ and η are the mass density and dynamic viscosity of the corresponding medium, p the scalar field of hydraulic pressure, and $\boldsymbol{u}$ the vector field of flow velocity. $\boldsymbol{F}$ represents any external body force acting on the fluidic system.

Ignoring the influence of the positive pressure of the solution and the moving viscous force of the droplet deformation, the force balance at the phase boundary referred to the balance between the viscous shear stress, the surface gradient of the interfacial tension, and the local interfacial tension balance at the curved interface Laplace pressure:

$$\tau_{LM} = \nabla_t \gamma \tag{S7}$$

$$\Delta p \cdot \boldsymbol{n} = \frac{2\gamma}{R} \cdot \boldsymbol{n} \tag{S8}$$

where ∇_t is the operator of the surface gradient, Δp is the difference of static pressure between the conducting droplet phase and the buffer medium phase, R is the principal radius of curvature of the LM droplet.

The electric Marangoni shear stress is generated by the surface gradient of

interfacial tension:

$$\eta \cdot \frac{\langle \boldsymbol{u} \rangle}{R} = \frac{\partial \gamma}{\partial x} \tag{S9}$$

According to Eq. (3), the surface velocity of the LM mainly included the global velocity component $\boldsymbol{u}_{\text{globe}}$ caused by inherent charge and the local velocity component $\boldsymbol{u}_{\text{local}}$ at different locations.

$$\boldsymbol{u}_{\text{globe}} = -\frac{q_0 ER}{\eta} \tag{S10}$$

$$\boldsymbol{u}_{\text{local}} = -\frac{CE^2 R}{\eta} x \tag{S11}$$

However, when the LM was in contact with the floating electrode, the floating electrode and the LMD formed a unified electrical conductor. Under the action of the external electric field, the induced charges were generated on the surface of the graphite floating electrode. The induced charge on the surface of the LM presented a unipolar distribution, as shown in Fig.S3. The potential difference across the NDL and IDL were ΔV_1 and ΔV_2, respectively:

$$\Delta V_1 = -\frac{q_0}{C} \tag{S12}$$

$$\Delta V_2 = E(L/2 + R - x) \tag{S13}$$

where L is the length of the floating electrode in the *x*-direction.

Similarly, the LM surface velocity when in contact with the floating electrode can be obtained:

$$\begin{aligned} \langle \boldsymbol{u} \rangle &= -\frac{q_0 ER}{\eta} + \frac{CE^2 (L/2 + R - x) \cdot R}{\eta} \\ &= -\frac{q_0 ER}{\eta} + \frac{CE^2 (L/2 + R) \cdot R}{\eta} - \frac{CE^2 R}{\eta} x \end{aligned} \tag{S14}$$

The velocity of the surface included the global velocity $\boldsymbol{u}_{\text{globe}}$ and the local velocity $\boldsymbol{u}_{\text{local}}$:

$$\boldsymbol{u}_{\text{globe}} = -\frac{q_0 ER}{\eta} + \frac{CE^2 (L/2 + R) \cdot R}{\eta} \tag{S15}$$

$$\boldsymbol{u}_{\text{local}} = -\frac{CE^2 R}{\eta} x \tag{S16}$$

SI Appendix 4: Fluid pressure produced by Marangoni flow.

The distributions of the flow field under the voltage of 2 V were obtained by simulation, as shown in Fig.2(f) and (g). By comparison, it was found that the flow of Marangoni fluid on the surface of the LMD drove the flow of the solution. There was a maximum flow rate on the surface of the LMD, and a fluid vortex was formed in the

solution. However, the direction of fluid flow was opposite in the two states of separation and contact. Moreover, due to the fluid flow in the solution, the fluid pressure was generated on the surface of the LMD. With reference to atmospheric pressure, the relative fluid pressure distributions were obtained by simulation, as shown in Fig.S4. The relative pressure on the left side of the droplet was greater than that on the right side, and a pressure difference was formed on the surface, as shown in Fig.S4(a). As a result, the LMD moved towards the positive electrode driven by the pressure difference when the droplet was separated from the floating electrode. Conversely, when the droplet contacted the floating electrode, a pressure difference in the opposite direction was created by the fluid flow, as shown in Fig.S4(b). Under the action of the pressure difference, the droplet tended to be flat and moved away from the graphite electrode.

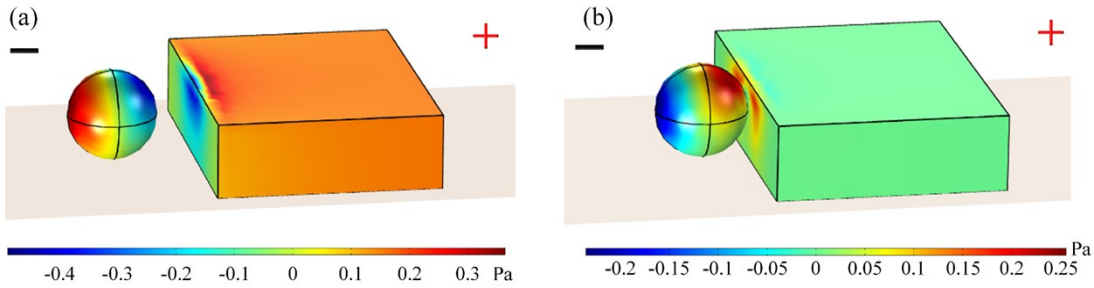

Fig. S4 The relative pressure on the LM and graphite produced by Marangoni fluid flow. (a) The distribution of relative pressure on the surface when the droplet was separated from the floating electrode. (b) The distribution of relative pressure on the surface when the droplet was in contact with the floating electrode.

SI Appendix 5: The influence of different factors on the heartbeat phenomenon.

A 100 μL LMD was placed in an open glass container with a length of 171 mm, a width of 83 mm, and a height of 20 mm, which was filled with the 2 mol/L NaOH solution. The volume of the NaOH solution was 40 mL, and the immersion depth of the droplet was 2.08 mm. And the distance between the two electrodes was 6 cm. A camera with 30 fps recorded the heartbeat phenomena under different voltages. Then the displacement and projected area change within 3 s were analyzed by ImageJ, as shown in Fig.S5. In this work, the displacement referred to the vertical distance from the center of mass of the LMD to the edge of the graphite, as shown in Fig.1(c). The projected area referred to the area of the LMD in the top view, as shown in Fig.1(d).

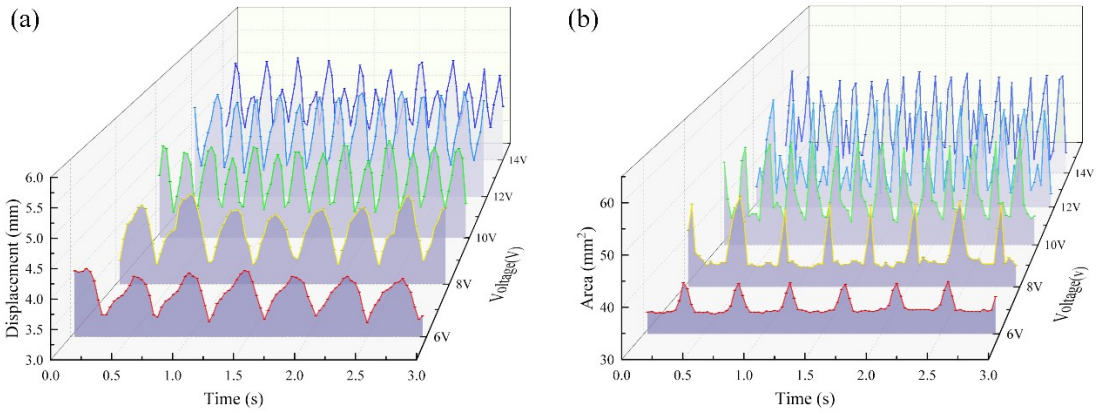

Fig. S5 The changes in the displacement and projected area under different voltages. (a) The changes in the displacement of LMD within 3 s under different voltages. (b) The changes in the projected area of LMD within 3 s under different voltages.

Under the 10 V voltage, the law of the heart beating with different electrode distances was studied. In the experiment, 100 μL droplet was put in the 2 mol/L NaOH solution. The volume of the NaOH solution was 40 mL, and the immersion depth of the droplet was 2.08 mm. The changes of displacement and projection area under different electrode distances were shown in Fig.S6.

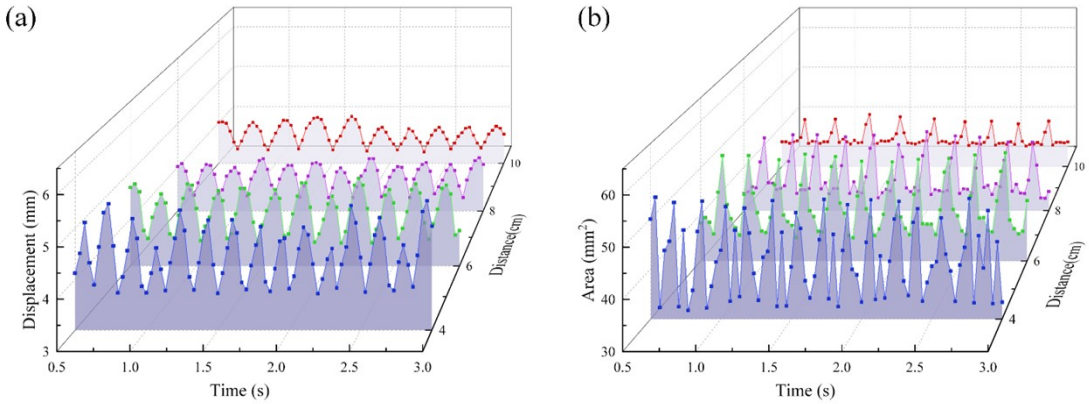

Fig. S6 The changes in the displacement and projected area under different electrode distances. (a) The changes in the displacement of LMD within 3 s under different electrode distances. (b) The changes in the projected area of LMD within 3 s under different electrode distances.

Then the heart beating phenomena of 100 μL droplet in 40 mL NaOH solution with different concentrations (immersion depth of 2.08 mm) were texted. In the experiment, a 10 V DC voltage was applied to the excitation electrodes, and the distance between the two excitation electrodes was 6 cm. The changes of displacement and projection area under different solution concentrations were shown in Fig.S7.

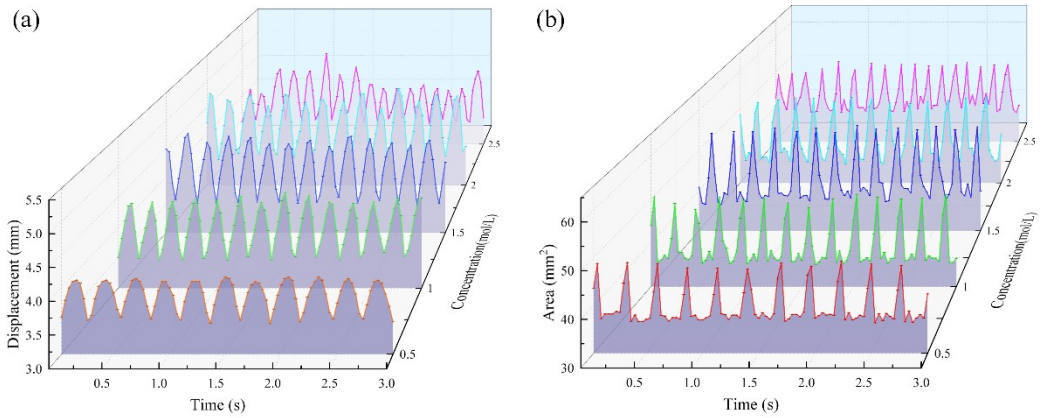

Fig. S7 The changes in the displacement and projected area under different solution concentrations. (a) The changes in the displacement of LMD within 3 s under different solution concentrations. (b) The changes in the projected area of LMD within 3 s under different solution concentrations.

Besides, the immersion depth of the droplet in the solution also had an impact on the heartbeat phenomenon. The immersion depth was adjusted by changing the volume of the NaOH solution (20 mL, 30 mL, 40 mL, 50 mL, 60 mL, and 70 mL). Here, 100 μL LMD was placed in the 1 mol/L NaOH solution, and a 10 V DC voltage was applied to the excitation electrodes. The distance between the two excitation electrodes was 6 cm. The changes of displacement and projection area under different immersion depths were shown in Fig.S8.

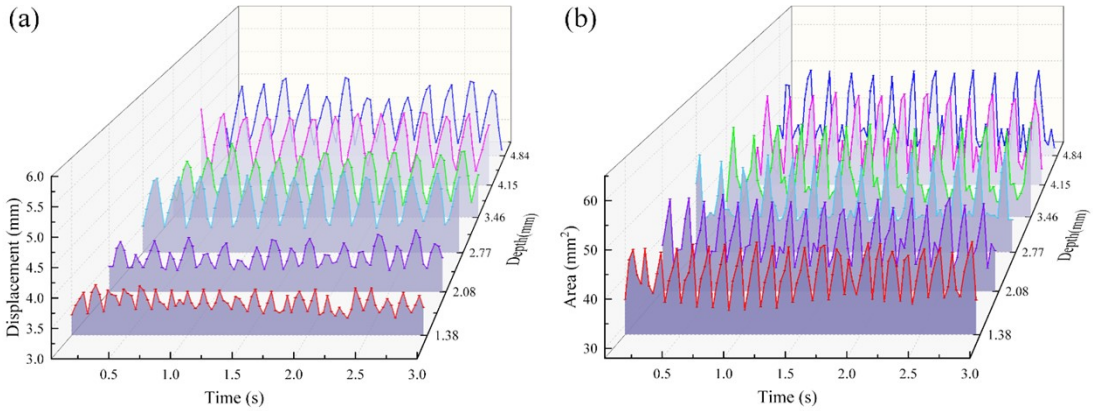

Fig. S8 The changes in the displacement and projected area under different immersion depths. (a) The changes in the displacement of LMD within 3 s under different immersion depths. (b) The changes in the projected area of LMD within 3 s under different immersion depths.

Moreover, different volumes of LMD showed different heartbeat effects in the 1 mol/L NaOH solution. The heartbeat phenomena of LMD of different volumes in the 40 mL NaOH solution were observed. 10 V DC voltage was applied to the excitation electrodes at a distance of 6 cm. The changes of displacement and projection area under different volumes of LMD were shown in Fig.S9.

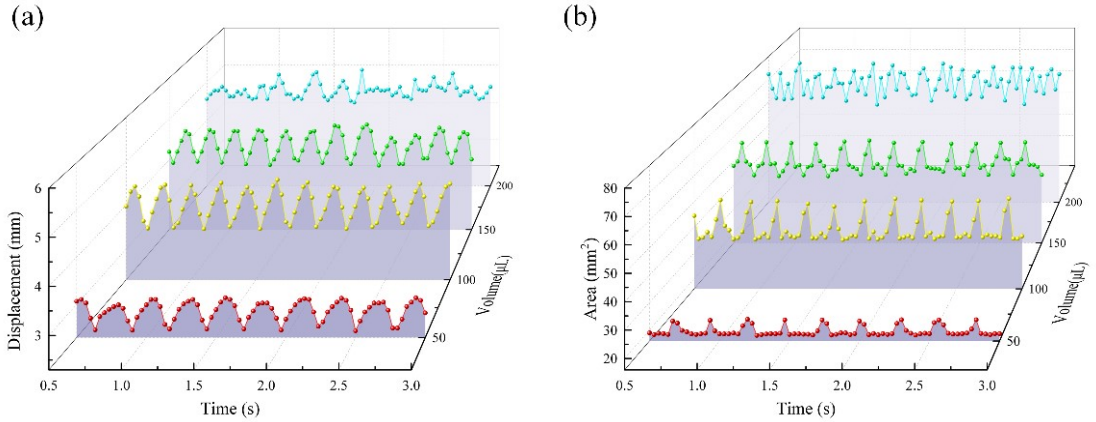

Fig. S9 The changes in the displacement and projected area under the different volumes of the droplet. (a) The changes in the displacement of LMD within 3 s under the different volumes of the droplet. (b) The changes in the projected area of LMD within 3 s under the different volumes of the droplet.

Finally, floating electrodes of different materials caused different heartbeat effects. The heartbeat effects of 100 μL LMD were investigated on graphite, copper, and iron floating electrodes, as shown in Fig.S10. During the experiment, the volume of NaOH was 40 mL and the concentration was 1 mol/L, the applied DC voltage was 10 V, and the distance between the two excitation electrodes was 6 cm.

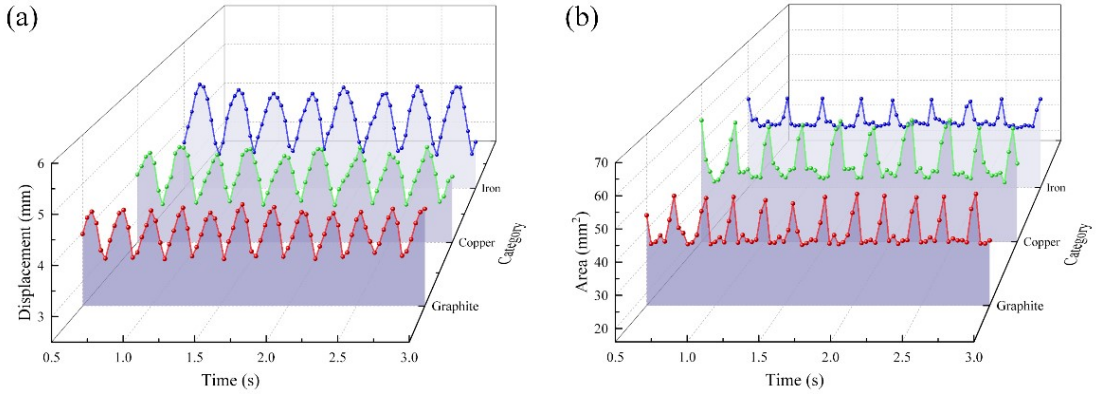

Fig. S10 The changes in the displacement and projected area under different types of floating electrodes. (a) The changes in the displacement of LMD within 3 s under different types of floating electrodes. (b) The changes in the projected area of LMD within 3 s under different types of floating electrodes.

The displacement difference Δx (shown in Fig.1(c)) of each heartbeat cycle was calculated and averaged, and this average value was considered as the final displacement difference. The calculation method of the projection area change ΔS (shown in Fig.1(d)) was similar to that of the displacement difference. Here, we expressed the change in projected area by the ratio of the changing area ΔS to the original area. Therefore, the influences on the heartbeat effect, such as the voltage, the volume of droplet, the immersion depth, the electrolyte concentration, the electrode distance, and the type of floating electrode, were analyzed in Fig.3.

SI Appendix 6: The reasons for the multi-frequency beating phenomenon.

The electric field intensity can be changed by adjusting the voltage and the electrode distance. However, when the intensity of the electric field continues to increase, the LMD no longer beats regularly at a fixed frequency. As shown in Fig.S11 (same as Fig. 4(f)), the displacement of LMD becomes unstable and loses regularity. Obviously, the three processes (chemical oxidation, chemical corrosion, and continuous electrowetting) of the heartbeat cross and overlap, as shown in the multi-frequency beating process in Movie S3. The chemical oxidation process is too fast and the oxide film is formed quickly. As a result, the isolation and separation of the LMD from the floating electrode occur in advance, which further causes the chemical corrosion process to proceed in advance, as shown in box A in Fig. S11. Therefore, the LMD has no time to deform to reach the maximum displacement. In addition, the fluid flow velocity and the driving force increase with the increase of the electric field intensity, so that the droplet starts to move to the positive electrode without the end of the chemical corrosion process, as shown in box B in Fig. S11. Clearly, the LMD enters the next heartbeat cycle without fully regaining its spherical shape. Finally, as the liquid metal heartbeat phenomenon becomes disordered, the multi-frequency beating phenomenon appears.

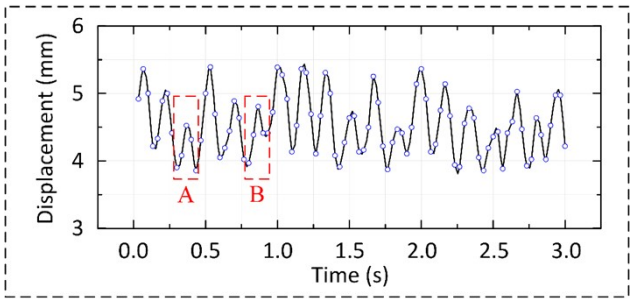

Fig. S11 The displacement changes of LMD when the multi-frequency beating phenomenon occurs.

SI Appendix 7: Pumping phenomenon on the surface of LMD.

When the voltage exceeded the cut-off voltage, the pumping phenomenon occurred on the surface of LMD. The LMD became long worm-like, as shown in Fig.S12. It was found that the fluid flowed from the positive electrode to the negative electrode by using ink to trace the direction. Two fluid vortices were formed on both sides of the liquid metal, thus driving the solution to form a circulating flow.

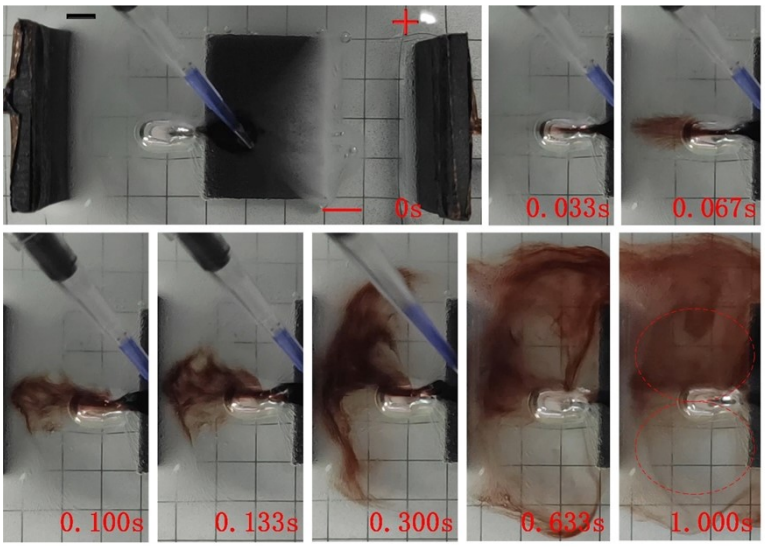

Fig. S12 Sequence chart of the pumping process.